We are IntechOpen, the world's leading publisher of Open Access books Built by scientists, for scientists

6,900
Open access books available

185,000
International authors and editors

200M
Downloads

Our authors are among the

154
Countries delivered to

TOP 1%
most cited scientists

12.2%
Contributors from top 500 universities



WEB OF SCIENCE™

Selection of our books indexed in the Book Citation Index in Web of Science™ Core Collection (BKCI)

Interested in publishing with us?
Contact book.department@intechopen.com

Numbers displayed above are based on latest data collected.
For more information visit www.intechopen.com



8

Synthesis and Properties of Discontinouosly Reinforced Aluminum Matrix Composites

Dusan Bozic and Biljana Dimcic
Institute of Nuclear sciences "Vinca" University of Belgrade
Serbia

1. Introduction

Due to the very high performance requests, a new type of, so called, "high tech" materials which are used in aircraft, rocket or automobile industry, need to have a good combination of properties under static and dynamic loading. One group of materials that can meet such requirements are metallic composites which consist of the metallic matrix (metal or alloy) reinforced whit whiskers or directionally oriented fibers of secondary phase.
Currently, there are many different composite materials available, enabling one to easily select the most suitable combination of metallic matrix and reinforcing phase, depending on the uniquely defined application requests. By selecting proper type of matrix and suitable chemical composition, shape and the amount of reinforcing phase, many composites with different mechanical properties can be produced. Potential application of such materials is very wide, but the limiting factor is still their quite high price due to the complexity of their production.
In the last two decades there was an intense development of one class of composites with aluminum alloy matrix best known as the discontinuously reinforced aluminum materials (DRA). These materials consist of aluminum alloy matrix reinforced by ceramic particles. Although, DRA composites can be produced in many ways, powder metallurgy technique offers the best results.
This article presents results of both fundamental and development studies of sintered composite materials with the Al-Zn-Mg-Cu matrix and the SiC reinforcing phase, conducted in last couple of years. As this is the composite which is already commercially applied or on the verge of being applied, all gathered results are thoroughly analyzed from the aspects of its synthesis, microstructure and several mechanical and fracture properties.

2. Matrix properties of sintered DRA materials

Mostly used alloys in the aircraft industry belong to the Al-Zn-Mg-Cu system. Usually in these alloys, traces of transient elements (below 1 mass %) such as: Fe, Si, Co and Ni can also be found. Commercially these alloys are known as 7000 or 7xxx class. One that has been used for this study is best known as CW67 alloy. Compared to the Aluminium alloys of the same composition produced by different techniques (such as melting and casting), sintered alloys have much better properties such as strength, fracture toughness and stress corrosion resistance (Tietz & Palmour, 1986). Mentioned advantages of these alloys can be related to the high amount of fine secondary precipitates and undiluted dispersed particles.

It is known that the phase particles which consist of elements such as Co or Fe+Ni are less prone to coarsening than the particles consisting of Cr, Ti or Mo (Tietz & Palmour, 1986). Precipitating phases Co_2Al_9 and $FeNiAl_9$, which are formed in the Al-Zn-Mg-Cu alloy, are very fine, ranging from 0.05-2 μm in size.Even finer particles can be produced by forming the dispersed oxide phase due to presence of oxygen (0.05-0.08 mass %) in this type of alloy.

Increased stress corrosion resistance of sintered DRA is favored by adequate grain morphology and presence of the higher amount of Co_2Al_9 precipitates in the structure. Presence of higher amount of Co has a very big influence on the higher fatigue resistance values of sintered alloys compared to casted ones (Tietz & Palmour, 1986). In order to obtain finer and more stable structure, a small amount of elements, such as Zr (0.2-0.8 mass %) can be added. Within casted alloys, amount of Zr cannot be higher than 0.12 mass %.

For further improvement of mechanical properties of sintered aluminum alloys, mechanical alloying can be applied (Tietz & Palmour, 1986). By performing mechanical alloying, multiple strengthening effects can be achieved: strengthening of the solid solution (commonly with Mg as an alloying element), precipitation strengthening and dispersed phase strengthening. It has been found that higher stress corrosion resistance of mechanically alloyed alloys of 550 MPa and high value of the Young's modulus of 76.5 GPa compared to other sintered alloys with values of 310 MPa for the stress corrosion resistance and 73GPa for the Young's modulus, make these alloys very interesting candidates for the further development and characterization.

Improvement of many properties (strength, Young's modulus, toughness etc.) of sintered Al-Zn-Mg-Cu alloys compared to the casted ones is achieved by using the contemporary powder metallurgy techniques. Production of alloy powders by rapid cooling process (rate of cooling in the range from 10^4 to 10^9 K/s), vacuum degassing of powders or compacts and powder compacting at elevated temperatures (hot pressing) are just a few of mentioned powder metallurgy techniques which can improve alloy properties (Figure 1).

An initial powder which is used for the production of sintered aluminium alloys can be made by several techniques, but mostly used one is pulverization. This technique is equally used in industry and smaller laboratories and there are several different types of it (Figure 2): gas atomization, ultrasound gas atomization, splat quenching, melt spinning *etc.* (Tietz & Palmour, 1986).

As it can be seen from the Fig.1, there are two mostly used compaction processes. Both processes consist of several steps. The first one starts with encapsulation, followed by powder degassing ending with compaction at higher temperatures (Tietz & Palmour, 1986). In the second process, powder is iso-staticaly pressed up to 70% of the theoretical density, degassed and only afterwards compacted at high temperatures up to theoretical density (Bozic et al., 1997). Both of these production processes are widely used, but the first one is more complicated (due to encapsulation/decapsulation), while the second one is less effective in removal of hydrogen and oxygen originating from the absorbed moisture in hydrated aluminum oxides. Degassing temperatures are in both cases in the range from 400 to 500 °C. Powder compaction at elevated temperatures (up to 500 °C) is done by hot pressing, hot iso-static pressing or hot extrusion which is mainly used for the production of the final products. By hot pressing at 450 °C during 2h and applied pressure of 35 MPa, a pore free compact can be produced (Fig. 3).

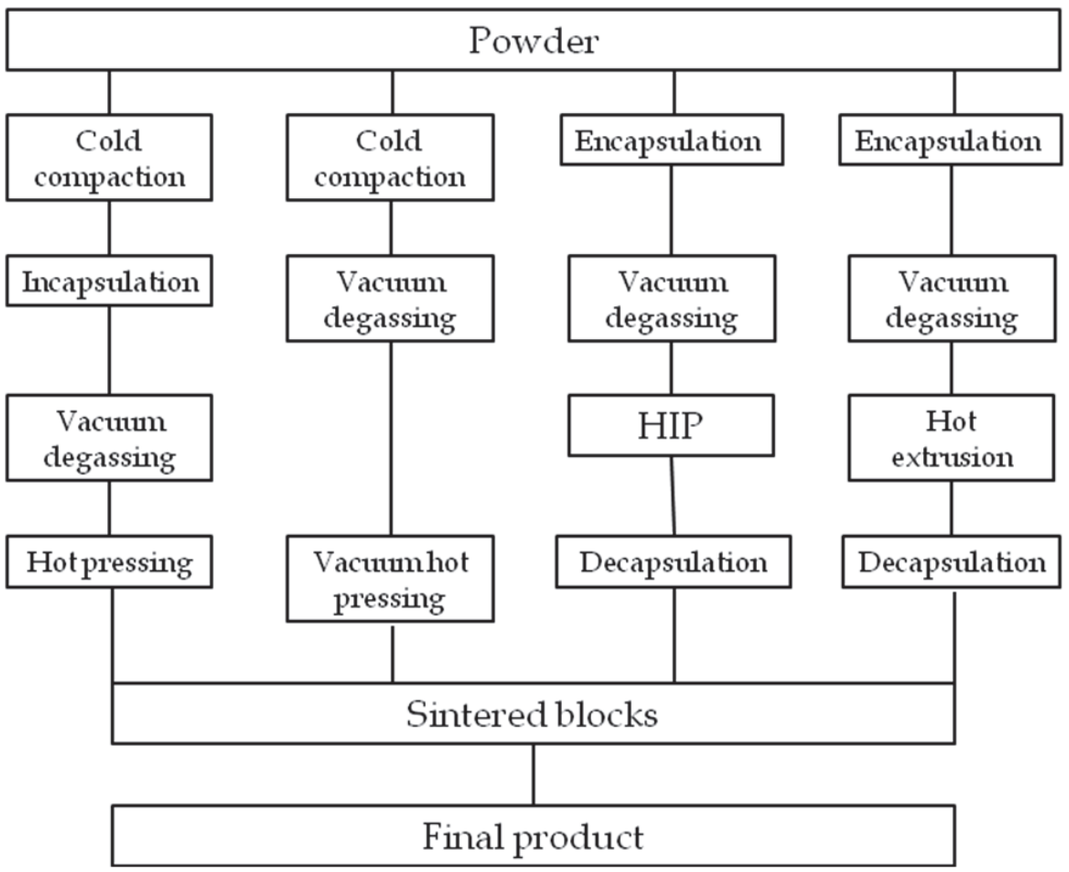


Fig. 1. Schematic presentation of high strength aluminum alloys production techniques (Tietz & Palmour, 1986).

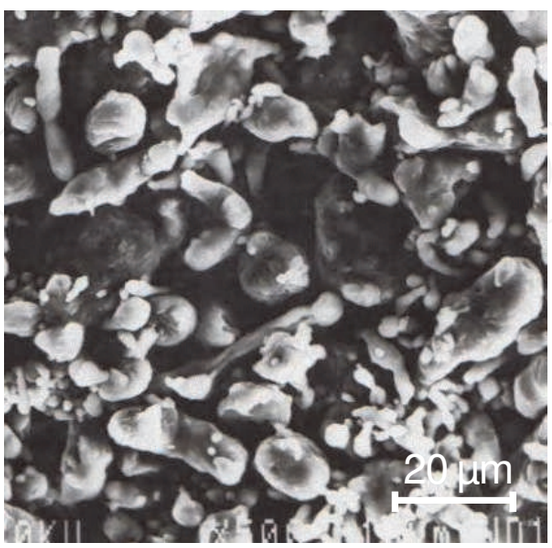


Fig. 2. SEM. Aluminum alloy powder (CW67) produced by gas atomization.

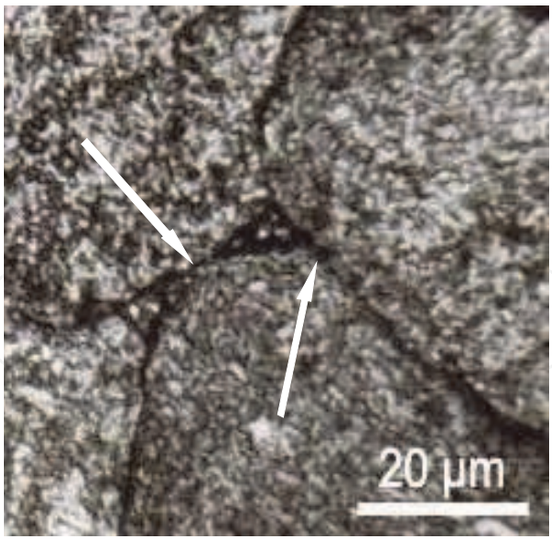


Fig. 3. SEM. Microstructure of hot-pressed Al-Zn-Mg-Cu alloy. Arrows denote a few prior particle boundaries.

Primary particle boundaries can be seen in the microstructure of the hot pressed compacts (arrows in Fig. 3), and most of the unwanted oxides which are deteriorating mechanical properties of the materials are located at these places (Gnjidic et al., 2001). Therefore, it is necessary to deform these materials by hot extrusion or rolling before use for the high risk applications (Bozic et al., 1997).
Since the Al-Zn-Mg-Cu alloy matrix is the precipitation strengthened alloy, it is important to perform adequate thermal treatment of the alloy after compaction. This treatment consists of the solution annealing at 475°c for 1h followed by water quenching and further ageing at 120°C for 24h or 160°C for 16h.
Mechanism of the thermally induced precipitation in Al-Zn-Mg-Cu alloys with the high Zn : Mg ratio can be presented in this way:

Saturated solid solution - Gunier-Preston (GP) zones - μ′ ($MgZn_2$) - μ($MgZn_2$)

Gunier-Preston (GP) zones are precipitating from the saturated solid solution, and they have coherent interfaces with the parent phase. Semi coherent μ′ ($MgZn_2$) phase has the monoclinic type of the crystal lattice, while the stable μ($MgZn_2$) phase has the hexagonal crystal structure. These phases are precipitating at different temperatures in the different time interval. When GP zones and the small amount of μ′ ($MgZn_2$) are present in the structure, alloy exhibits the highest strength values. Addition of Cu above 1 mass % can also increase the strength (strengthening due to alloying) but the precipitating mechanism still remains the same. When there is more Cu in the chemical composition of the alloy, it can be involved in the precipitation by replacing the Zn atoms.

3. Reinforcing phase properties of sintered DRA materials

Selection of an appropriate composition, morphology and volume fraction of reinforcing phase is a matter of trade off between the requested mechanical properties and its economic value. Typical properties which have the biggest effect on the selection of the particular

reinforcing phase are: Young's modulus value, wear resistance, fracture toughness, fatigue resistance and thermal expansion coefficient. A proper choice of the type and geometry of the reinforcing phase is very important for achieving the best combination of required properties and costs.Mostly used reinforcing phases for the production of discontinuously reinforced composites are: SiC in the shape of whiskers, particles of SiC or Al_2O_3, short Al_2O_3 or graphite fibers. Compared to fibers, particles and whiskers are easier for production; they are less expensive and have stable properties.

Whiskers are monocrystalline materials with a high length/width ratio (50 to 100). This shape of reinforcing phase is mostly used for composites that will be submitted to extrusion, rolling or forging. Unlike the particle reinforced composites, materials reinforced with whiskers are slightly less isotopic and their price is much higher.

Reinforcing phase in particle shape is not very expensive. Maximal/minimal particle dimension ratio is quite low (1 to 5). They have more isotropic properties compared to whiskers, resulting in better characteristics of composite materials. This property enables obtaining better characteristics of composite materials. It is important to know that this type of reinforcing phase is most commonly made by conventional methods used for the production of the metallic materials as well.

Technical SiC, which is mostly used as a particle reinforcing phase is often produced by reaction between SiO_2 and coke (in excess amount). SiC powder obtained in this way may still contain a small amount of un-reacted SiO_2 or free graphite (Fig. 4). Free graphite in a SiC powder can reduce the mechanical properties of the composites and therefore it has to be removed. Removal of this graphite can be done by thermal treatment of the powder at 900 °C for 2h (Gnjidic & Bozic, 1999).

Unlike composites produced by melting and casting that consist of particles with dimensions of hundreds of microns, composites produced by powder metallurgy techniques can use only much finer particles. Usual size of the SiC particles lies in the range from submicron size up to around 20 μm (Figs. 5-7).

As it can be seen from the images, SiC powder characteristics can differ depending on its particle shape, which can be: spherical (Figs. 5 and 6), polygonal (Fig. 6) or irregular with sharp edges (Fig. 7). In submicron powders, appearance of the agglomerates is common (Figs. 5).

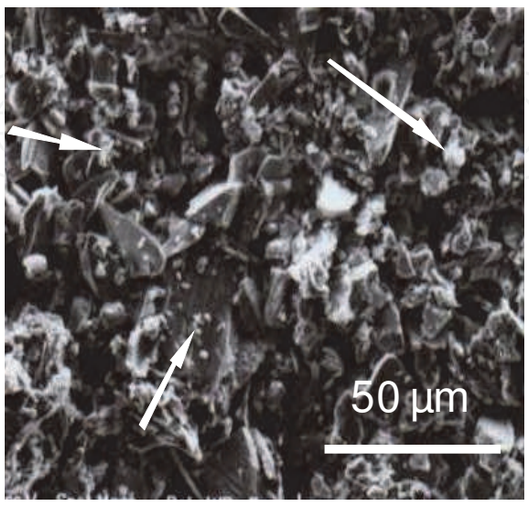


Fig. 4. SEM. SiC powder particles before heat treatment. Arrows appointing free graphite.

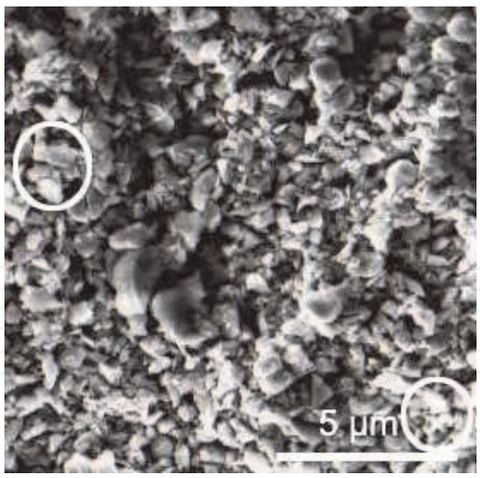


Fig. 5. SEM. Size and shape of SiC powder particles (average size 0.7 µm). Circles denote agglomerates.

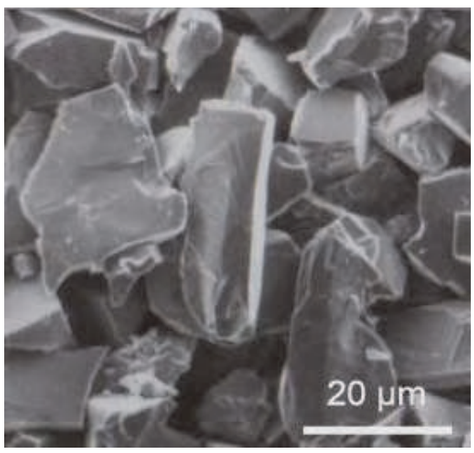


Fig. 6. SEM. Size and shape of SiC particles (average size 10 µm).



Fig. 7. SEM. Different shapes of SiC particles (average size 15 µm).

4. Mixing process

Mixing or homogenization of powders is one of the most critical processes in production of DRA materials by powder metallurgy techniques. If it is done properly, particles of the reinforcing phase can be uniformly distributed in the composite metallic matrix which improves the structural and mechanical properties of these materials. The most important parameters that influence effectiveness of the mixing process are: mixing dish filling rate, rotation velocity and mixing time (German, 1994). Optimal values of these parameters are mostly confidential or patent protected. This means that for every combination of powders (shape, size, amount of reinforcing phase) and mixing dish type it is necessary to experimentally find optimal mixing conditions, *i.e.* optimal values of the previously mentioned parameters.

One method for quantitative analysis of the SiC particle distribution homogeneity is based on the concept of homogeneity index, Q, which is a quantitative measure of the one component powder particle distribution homogeneity in the mixture of a few powders (Gray, 1973). It should be noted that this concept can only be valid under assumption that the volume fraction of the observed particles is equal to their surface fraction.

Standard deviation (α) of particle surface measurements is defined by Eq. (1):

$$\alpha = \frac{1}{N}\sum\left|A_i - A_f\right| \tag{1}$$

Where N is the number of repeated measurements, A_i is the individual area fraction and A_f is the mean value of all measured particle surfaces.

Equation (2) describes the case in which completely separated system appears (complete segregation) or, in other words, system in which the whole measuring surface belongs to the particles of just one powder component.

$$\alpha = 2A_f(1 - A_f) \tag{2}$$

By combining Eqs. (1) and (2), homogeneity index, Q, can be calculated as:

$$Q = \alpha/\alpha_{seg} \tag{3}$$

Values of homogeneity index vary from 0 (perfect uniform distribution of particles in the mixture) to 1 (complete non-uniformity of the powder particles).

Using this method, a homogeneity index for all mixtures can be determined by analyzing the eight randomly chosen measuring fields split into 16 measuring units. The size of the measuring unit can be calculated from the Eq. (4):

$$A = 1/N_A \tag{4}$$

Where N_A is the number of SiC particles in the measuring unit.

By using any type of software for the quantitative analysis of the microstructure, homogeneity of SiC particle distribution in metal matrix can be calculated (Mc Kimpson et al., 1999).

In our study, which is based on the data found in the literature (German, 1994), mixing dish rotation velocity was taken to be constant and equal 70 rpm for all regimes. Beside the rotation velocity, mixing time of 30 min was taken as a constant for the first five regimes as

well. The amount of powders was different and it was increased by 5 vol. % for each following regime. In the second five regimes, mixing dish filling rate was kept constant while the time of mixing was changed. The selected mixing dish filling rate was the optimal value from the first five experimental regimes (Table 1).

Mixing of powders occurred due to 'diffusion" in the cylindrical dish without any mixing accelerators. Results of quantitative microstructural analysis showing the effect of the mixing dish filling rate on the homogeneity index values are presented in Fig. 8.

All mixtures were well mixed and differences between their homogeneity indexes were in the range of 15%. Dependence of homogeneity index on the mixing dish filling rate for three different volume fractions of SiC particles in the mixture exhibits the same trend. The optimal value was achieved for the mixture with the lowest amount of the reinforcing phase.

The resulting force that affects particles in powder mixture during mixing is a result of unified influences of centrifugal, gravitational and frictional forces.The latter one exhibits the predominant effect on the mixing (homogenization) results. It was found in this study that optimal mixing dish filling rate was the lowest one (20 vol. %). The reason for this might be the fact that inter-particle contact is minimal during mixing since the available length for the free fall of particles is maximal, and therefore, agglomerates are hard to form and the ones already formed can easily be destructed (Fig. 8). With increase of the mixing dish filling rate, amount of SiC powder also increases forming more agglomerates that need to be destroyed. Available length for the free fall of particles also decreases resulting in overall decrease in powder mixture homogeneity. Negative effect of agglomerate presence in the microstructure can also be increased with the increase of SiC particle amount. It is known that a very large number of parameters influence the efficiency of particle stacking in the volume of the powder (Gray, 1973). The most important parameters are shape, size, physical and chemical characteristics of the powder particles as well as the shape, size and material of the mixing dish and many more. The real influence of only one parameter is very hard to predict since it often overlaps with the influence of another one. In the case of heterogeneous system there is one additional parameter and that is the volume fraction of the second powder. Higher amount of additional powder decreases the efficiency of particle stacking but not very dramatically since homogeneity indexes do not differ much between the different analyzed mixtures (Fig. 8).

Regime	Mixing dish filling rate (vol. %)	Mixing time (min)
I	20	30
II	25	30
III	30	30
IV	35	30
V	40	30
VI	30	60
VII	30	90
VIII	30	120
IX	30	150

Table 1. Different mixing regimes for metallic-ceramic composites

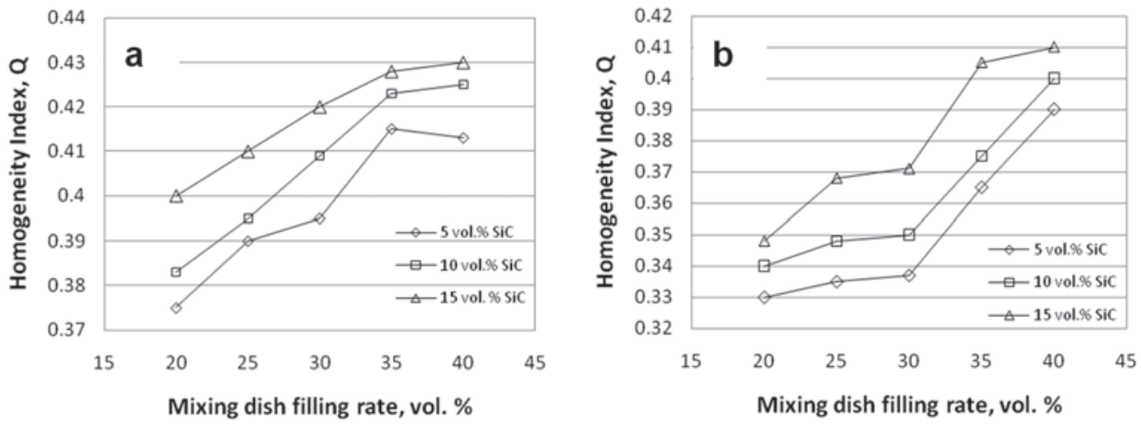


Fig. 8. Plot of homogeneity index values *vs.* amount of the mixing dish filling rate for alloys with a) 0.7 μm and b) 15 μm sized reinforcing powder particles.

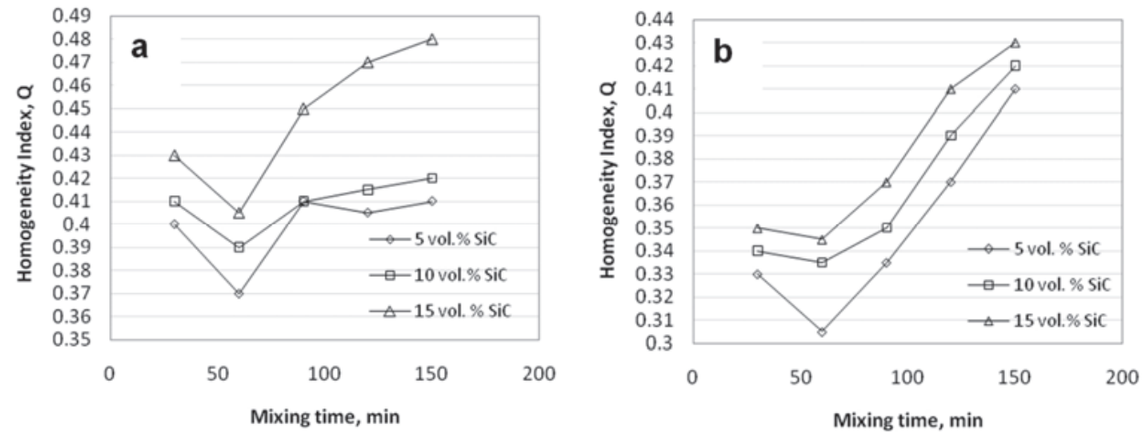


Fig. 9. Plot of homogeneity index values *vs.* mixing time for alloys with a) 0.7 μm and b) 15 μm sized reinforcing powder particles.

It can be noticed from Fig. 9 that influence of the mixing time on the homogeneity index values is much higher than the influence of the mixing dish filling rate (Fig. 8). Values of homogeneity index increase up to 40% with the increase of mixing time compared to the optimal one.

Plots of homogeneity index values *vs.* mixing time, for the optimal value of mixing dish filling rate, exhibit the same trend for all mixtures. The best homogeneity is, like in the previous case (Fig. 8), obtained for the mixtures with 5 vol. % SiC. Mixing time of 60 min was optimal from the aspect of secondary (reinforcing) phase distribution. It is known that during longer mixing time the effect of particle "diffusion" is more pronounced (German, 1994). All plots display the increase of homogeneity index with increase of the amount of reinforcing phase in the mixture during constant mixing time. That kind of behavior is somewhat expected because of increase of the number of reinforcing phase particles that need to be mixed. Figs. 10 a-c and 11 a-c display the microstructures of samples with the optimal homogeneity which are produced under the optimal mixing conditions. Figs. 10 d

and 11 d illustrate so called diffusion mixing as a result of prolonged mixing time. Scanning electron images clearly show clusters of SiC as well as areas without SiC presence.

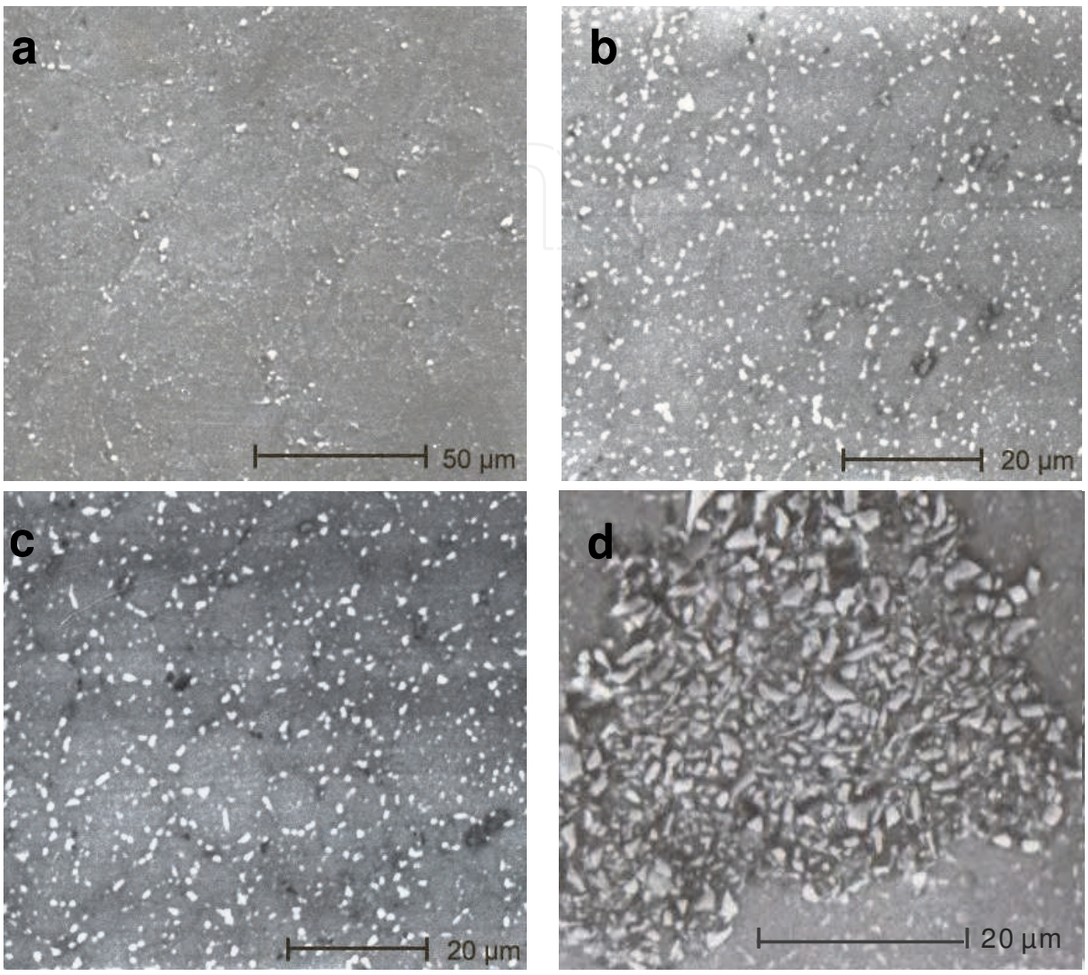


Fig. 10. SEM. Composite microstructure (d_{SiC}=0.7 µm)-optimal homogeneity. a) 5 vol. % SiC, b) 10 vol. % SiC, c) 15 vol. % SiC, and example of prolonged mixing time effect, d) 15 vol. % SiC, 150 min mixing time.

SiC powder with medium size particles of 15 µm, used in this study is characterized by wider particle size distribution. Around 20 mass.% of this granulation contained particles larger than 20 µm, and a certain percent of 1-2 µm sized particles. Several authors (Flom and Arsenault, 1989) found that when a SiC particle size is 20 µm or larger, fracture process changes from mainly matrix controlled failure to particle cracking controlled. On the other hand, particles of around 1 µm are often prone to agglomeration during mixing. Therefore, even under optimal mixing conditions, segregation of particles, presence of surface defects and cracking of large particles can be expected with this kind of reinforcing material.
By sieving this fraction, a powder with the medium size SiC particles of 10 µm, characterized by the considerably narrower particle size distribution than the previous one can be extracted, Fig. 6.

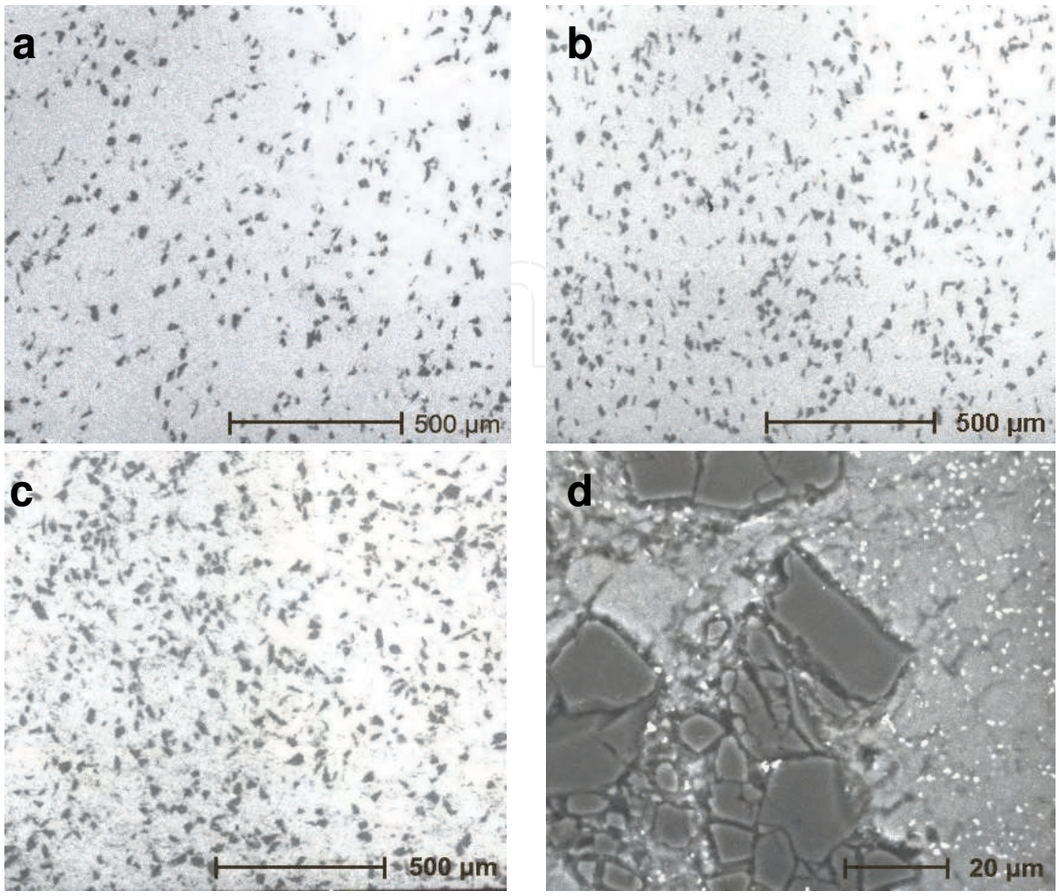


Fig. 11. LM. Composite microstructure (d_{SiC}=15 µm). a) 5 vol. % SiC, b) 10 vol. % SiC, c) 15 vol. % SiC, and example of prolonged mixing time effect, d) SEM. 15 vol. % SiC, 150 min mixing time.

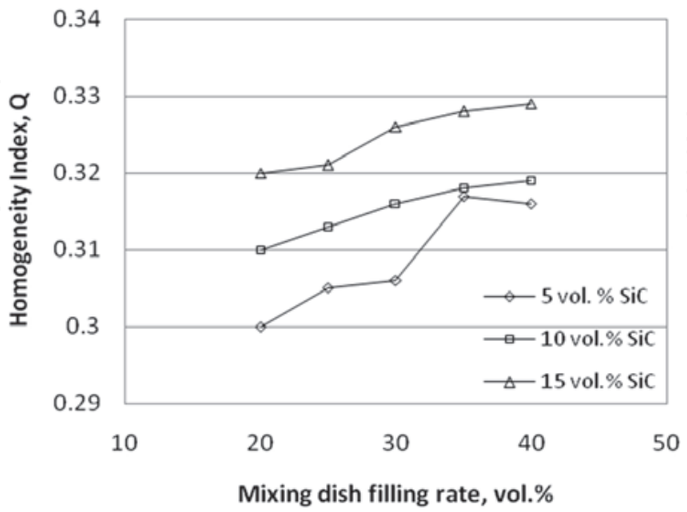


Fig. 12. Plot of homogeneity index values *vs.* mixing dish filling rate for the alloys with 10 µm size reinforcing phase particles.

Mixing of aluminum alloy and SiC powders was conducted under the same conditions as in the previous cases in this study. Dependence of the homogeneity index on the mixing dish filling rate and mixing time is shown in Figs. 12 and 13. Although the character of the plots is similar to the previous ones in Figs. 8 and 9, we can see some differences. In this case, higher degree of homogenization is achieved and better distribution of reinforcing particles is observed even for longer mixing times. Microstructures of such mixtures are presented in Fig. 14 a and b.

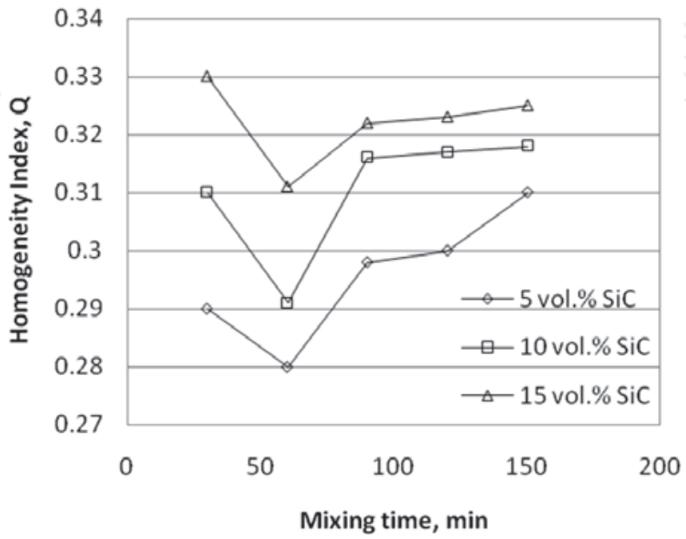


Fig. 13. Plot of homogeneity index values *vs.* mixing time for the alloys with 10 μm size reinforcing phase particles.

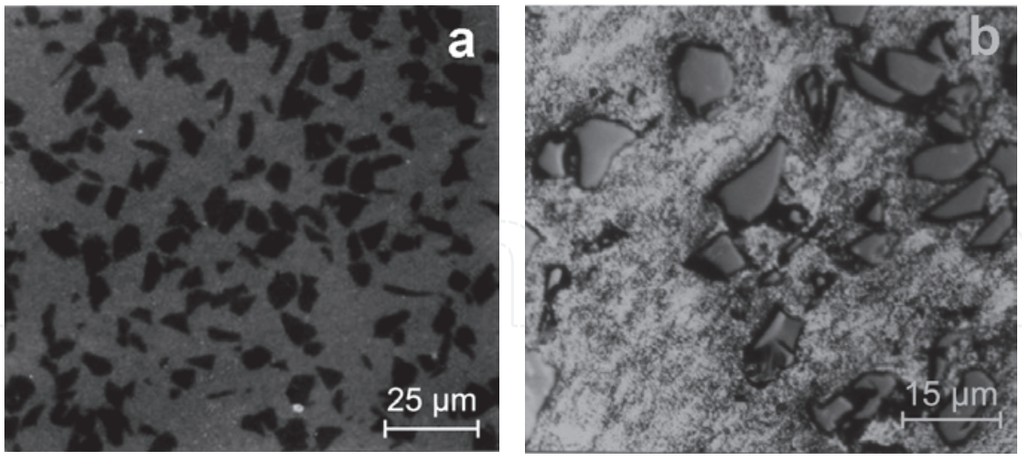


Fig. 14. Composite microstructure (d_{SiC}=10 μm). a) LM. Optimal homogeneity reached-15 vol.% SiC and b) SEM. Effect of prolonged mixing time -10 vol.% SiC.

Different values of mixing dish filling rates and mixing time have great influence on the SiC particle distribution in aluminum alloy and hence on the mechanical properties an mechanical behavior of the produced DRA material.

5. Methods of powder mixture consolidation

In order to make a fully dense product, powder mixture needs to be consolidated. Powder metallurgy consolidation techniques consist of three basic steps:

1. Cold isostatic pressing (CIP) - enables formation of compacts with density of 65-75% of the theoretical density;
2. Compacts degassing at high temperatures-removal of absorbed gases and moisture;
3. Hot or hot vacuum pressing, hot iso-static pressing or hot extrusion -production of compacts with theoretical density.

Existence of the open porosity in compacts after cold iso-static pressing enables further vacuum degassing. Degassing temperature is usually in the range from 400 to 500˚C. Incomplete degassing results in detaining a large amount of oxides on the particle surface which cause weaker particle bonding in the following stages of consolidation process. In this kind of material, formation of cracks and fracture along the primary particle boundaries is likely to occur. On the other hand, too high degassing temperatures or very long degassing times are not very favorable since they can lead to decrease of the Zn amount in the composite matrix (in 7000 alloys).

Mostly used consolidation techniques for production of DRA materials are hot pressing and hot vacuum pressing. Difference between these two is that in the first case mixture of powders or porous compact is encapsulated, degassed and then hot pressed in air, while in the second case degassing is done without encapsulation of the material just before the hot pressing under vacuum. It is accepted that the latter one offers better results.

To control a large number of parameters and to understand certain mechanisms of above mentioned processes is very important for the production of composites. By presenting the densification process with densification maps it is much easier to comprehend these issues (German, 1996). Practical value of these maps is that they link the influence of the crystal structure and atomic bonds on the plastic flow of the materials. This further enables more simple analysis of mechanisms which are very important for the experiment design.

Densification maps presented in Figure 15 (Bozic et al., 2009) are determined for the constant pressure of 35 MPa and for the constant size of matrix powder particles (2R=125 μm). A model that is used is universal and it allows the comparison of densification mechanism for different applied pressures and different particle sizes. Other densification process parameters can easily be changed by changing boundaries between zones of dominating densification mechanisms. Due to the modular model structure, complete modulus can be corrected or changed. This fact is particularly useful since it enables potential corrections of the model.

A model used in this study was made for analyzing different densification mechanisms during the hot pressing, such as plastic flow, power-law creep and diffusion. From the chosen examples it can be noted that the process of densification is slowing down as the fraction of the reinforcing phase increases (slope of the dashed lines) which is in agreement with the experimental studies. A change in densification mechanism during hot pressing induced by the change of fraction of reinforcing phase can also be observed from this maps (different size of the zones for certain densification mechanism).

Densification maps provide a possibility of predicting dominant deformation mechanism, densification rate and time of pressing for the given conditions of hot pressing process.

Densification parameters are slightly changed compared to the optimal hot pressing parameters for the DRA materials production. Poreless structure was obtained at higher temperature (470 ˚C) and during longer time (5h). Only under these conditions densification can be fully performed when low pressure (35 MPa) is applied.
In the presented case, complete densification was achieved for aluminum alloy and DRA composite with 15 μm SiC, but not for the composite containing the smallest (0.7 μm diameter) SiC particles.

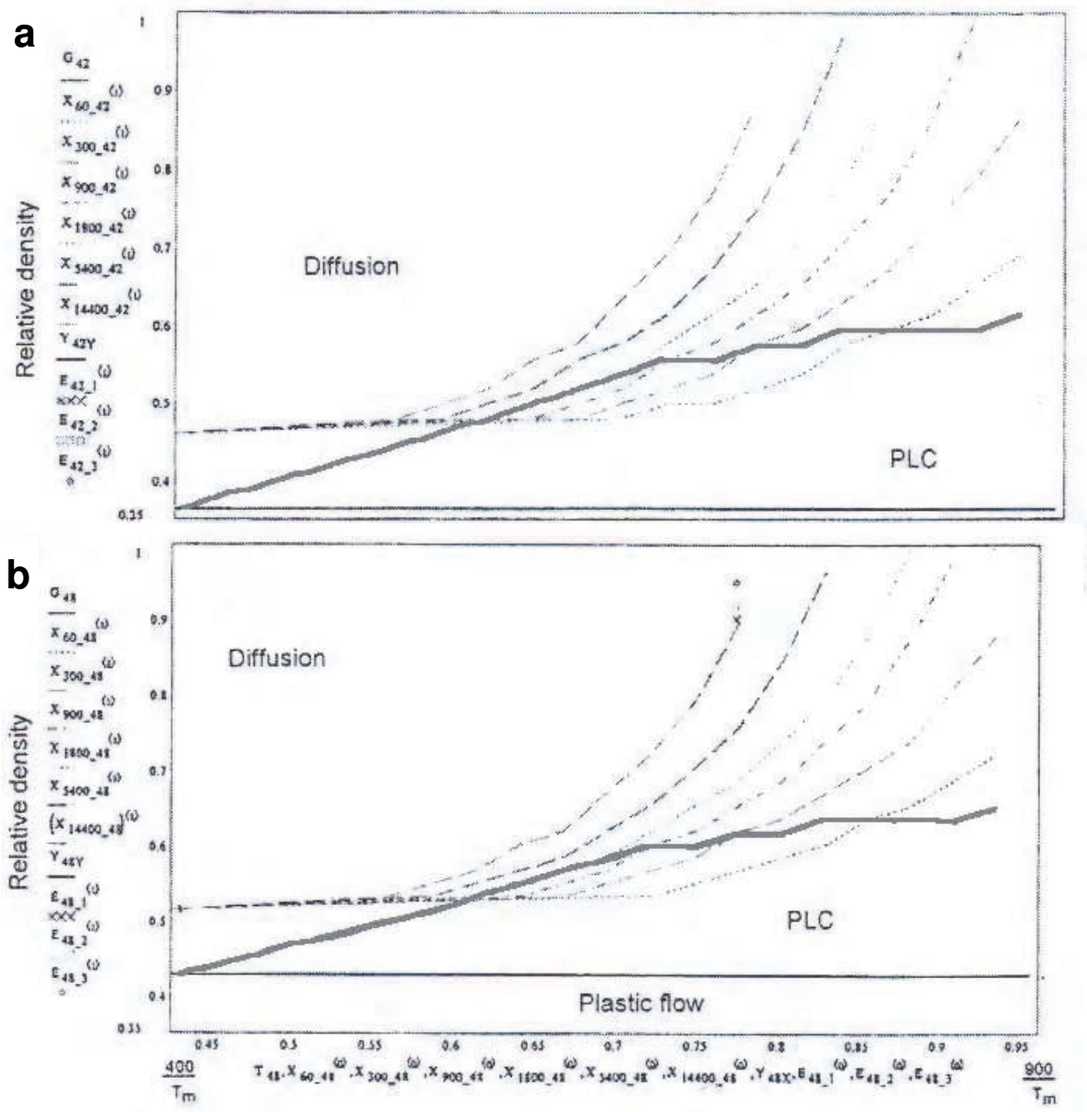


Fig. 15. Deformation mechanism maps (X_{t_D0} is a time curve, where t is the time of densification and D_0 is the starting density of the powder, and E_{D0_n} is the group of experimental values; thick line represents the boundary between power-law creep and diffusion zones. a) Pure Al powder; b) Al-10 vol.% SiC composite. Al particle radius in the composite was $2R=125\ \mu m$, and SiC particle radius was $2R=33\ \mu m$. Applied pressure was $P=35$ *MPa (Bozic et al*., 2009)

Microstructures of the hot-pressed composite materials show that mixing parameters used in the present work enabled formation of relatively uniformly distributed SiC particles in the aluminum matrix (Fig. 16 a and b). Porosity existing in the composites reinforced with 0.7 μm SiC, which has been detected after density measurements (Table 2) is illustrated in Fig. 17. Formation of agglomerates during mixing was the primary reason for such behaviour.

Sample	Theoretical density, ρ_t (g/cm^3)	Density, ρ (g/cm^3)	Percentage of theoretical density
CW67	2.88	2.87	100
CW67-0.7 μm SiC	2.90	2.80	97.5
CW67-15 μm SiC	2.93	2.93	100

Table 2. Density values of the hot pressed aluminum alloy (CW67) and two selected composites.

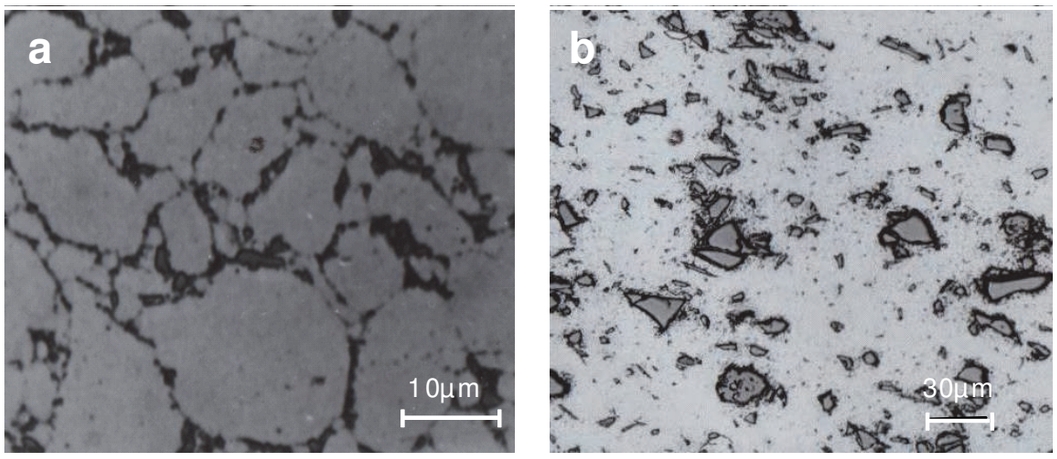


Fig. 16. Microstructures of hot-pressed samples. a) LM. Composite containing 10 vol.% - 0.7 μm SiC, b) SEM. Composite containing 10 vol.% - 15 μm SiC.

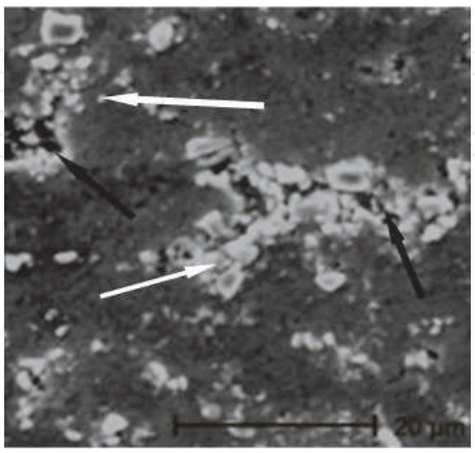


Fig. 17. SEM. Microstructure of hot-pressed composite containing 10 vol.% - 0.7 μ SiC. White arrows -particle agglomeration; Black arrows-pores.

6. Influence of the reinforcing phase on mechanical and fracture characteristics of DRA materials

Prior to compressive testing, all hot-pressed materials were subjected to two types of thermal treatments: under-ageing and peak-aging. Initially, all samples have been homogenized by solution thermal treatment (1h at 475 ˚C) followed by water quenching to room temperature. Under-ageing was performed at 120 ˚C for 1h, while the peak-ageing was done at the same temperature of 120 ˚C for 24h for the CW67 alloy and 22h for the composites. Presence of SiC particles significantly influences the heterogeneous nucleation of strengthening phases. Capability for heterogeneous nucleation can be partially attributed to high dislocation density in the composite matrix, which is present due to the large mismatch between the thermal expansion coefficients of the matrix and the reinforcing phase. It is well known that dislocations act as nucleating sites for precipitation during aging, but they also promote accelerated ageing in the matrix. For that reason, peak-aging conditions for composites are reached in shorter times than for the monolithic alloy (Fig. 18).

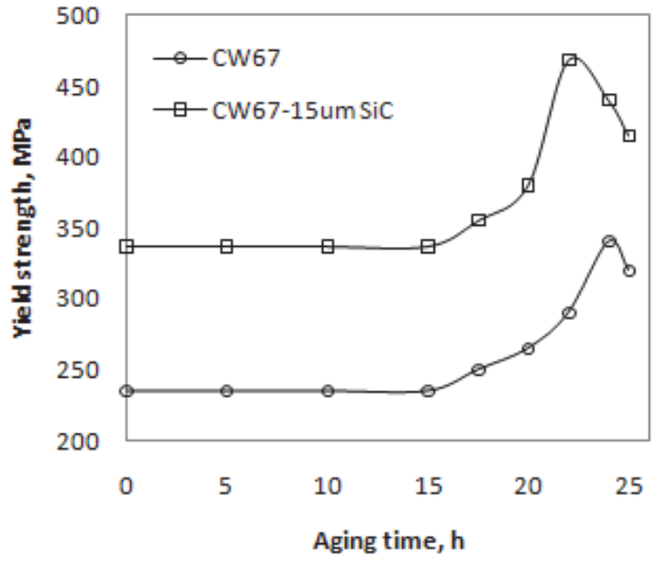


Fig. 18. Yield strength of the CW67 alloy and its corresponding composite *vs.* aging time.

Influence of different SiC particle sizes on the yield strength (σ_{yc}), ultimate strength (σ_{uc}) and ductility (strain to failure) (ε) under compression at room temperature for both under-aged (UA) and peak-aged (PA) samples is listed in Table 3.

Values of yield strength (measured at 0.2 % offset strain) for all composites, irrespective to heat treatment, are higher than those of the monolithic alloy. On the other hand, the ultimate strength and ductility values of the composite samples are lower than those obtained for the unreinforced alloy. It can also be noted that 0.2 % offset strain occurred at much higher fraction of the total strain-to-failure in the composite than it did in the case of the CW67 alloy. Main reason for such behavior could be the influence of the SiC particle sizes, their nature and agglomerate formation. These results also imply that smaller number of particles is damaged when the applied stress reaches yield stress in the composites. Stress will continue to accumulate after reaching the yield strength, leading to rapid failure and therefore low values of the ultimate strength and ductility.

Analysis of results indicates that the samples submitted to peak-aging generally exhibited higher yield strength and ultimate strength values but also lower ductility when compared to under-aged samples.
The highest compressive property values are obtained for the composite reinforced with 10 μm SiC particles. It is worth noting that the lowest values are obtained for the composite material with 0.7 μm SiC particles. This result is unexpected since it is known that particle size decreasing is associated with improved mechanical characteristics of the particle reinforced composites.

Material	σ_{YC} (MPa)		σ_{UC} (MPa)		ε (%)	
	UA	PA	UA	PA	UA	PA
CW67	235	340	860	950	38	35
CW67-0.7 μm SiC	312	400	720	740	22	19
CW67-10 μm SiC	400	490	850	930	27	23
CW67-15 μm SiC	331	437	743	830	24	20

Table 3. Compressive properties of pure aluminum alloy and reinforced materials in under-aged (UA) and peak-aged (PA) conditions.

Generally, mechanical behavior of composites is affected by the presence of reinforcing particles dispersed in the metal matrix. When analyzing the yield behaviour of these materials, it is important to recognize that the yielding strength of the composite is determined by the yield strength of the matrix. Most probably yield strength may not be the same as yield strength of the monolithic alloy processed and heat-treated in a similar way (Doel & Bowen, 1996). The local yield strength of the matrix may, in fact, be higher than that of the monolithic material due to the increased dislocation density and reduced grain size. Namely, matrix grain size is reduced by particles acting as nucleation sites during solidification. Also, grain size is smaller due to formation of subgrains after dislocation rearrangement into boundaries within the grain (Rees, 1998). These subgrains are formed in grains with high dislocation density surrounding a SiC particle. This rearrangement is a recovery process driven by the energy stored within the distorted matrix at the interface of two phases. Also, SiC particles act as obstacles for dislocation motion.
There are several factors affecting the local stress in the matrix. First of all, there is a tensile residual stress field in the matrix due to the difference in coefficient of thermal expansion (CTE) between aluminum alloy and SiC. Partial relief of this stress can result in an increase of dislocation density (Miller & Humphreys, 1991). Further, any applied load cannot be evenly distributed between the matrix and the SiC particles because of difference in stiffness. Several authors have previously reported that the reinforcing phase can support more applied load than the matrix (Doel & Bowen, 1996). Thus, local stress in the matrix may be lower than the nominal applied stress. In addition, SiC particles can withstand this stress until it becomes sufficiently high to cause particle fracture or failure either at or near the interface. It is believed that damage will first occur by particle fracture because the interface between SiC particles and aluminum is very strong. Hence, as soon as the particle breaks the stress in the undamaged material increases. In time, micro voids are beginning to

form in the matrix as a result of dislocation pile-up, due to the applied load. These voids continue to grow causing failure of composite materials.

In order to comprehend the exact influence of SiC particle size on the compressive properties of the composite, a comparison was made between the properties of three composites in both under-aged and peak-aged condition.

Composite sample with 0.7 μm SiC particle size had the smallest increase of yield strength, presumably due to the presence of the agglomerates in the structure (Fig. 17), originating from the starting powder (Fig. 6). In this case, matrix around the agglomerates is subjected to higher stress because they cannot support the same amount of stress as non agglomerated particles. Therefore, matrix is forced to yield at lower applied stress and, therefore, yield strength of the composites is also lower. Fracture surface of this composite show evidence of both trans-crystalline and inter-crystalline fracture mechanisms (Fig. 19). A factor that might have a detrimental effect on the compressive properties of this particular composite material is the homogeneity of the particle distribution.

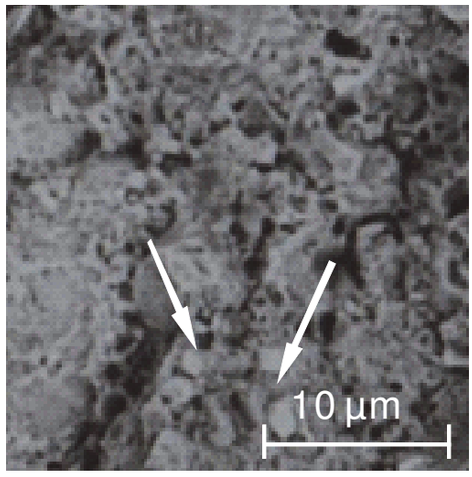


Fig. 19. SEM. Fracture surface of composite with 0.7μm SiC particles in peak-aged condition. White arrows appointing agglomerates.

Composites reinforced with 10 and 15 μm SiC particles are generally both stronger and more ductile than the material reinforced with 0.7 μm particles. Of the two analyzed composites, one containing 10 μm SiC particles has the highest increase in yield strength and the lowest decrease in ultimate compressive strength and ductility for both ageing conditions.

Main reason for the superior mechanical characteristics of the medium sized particles composites is uniformity of reinforcing phase particle dimensions (Fig. 20) and structure without agglomerates.

By making a mixture with narrower particle size distribution, the number of fracture initiation sites in DRA material is reduced making the matrix/SiC decohesion a dominant fracture mechanism (Fig. 20).

Formation of the crack and the crack path depend on the microstructure homogeneity of the alloys. Uniform path of the existing crack is typical for the less homogenous alloys, while the zig-zag path characterizes homogenous alloys (Fig. 21). The latter type of crack propagation is a consequence of homogenous distribution of secondary (SiC) particles

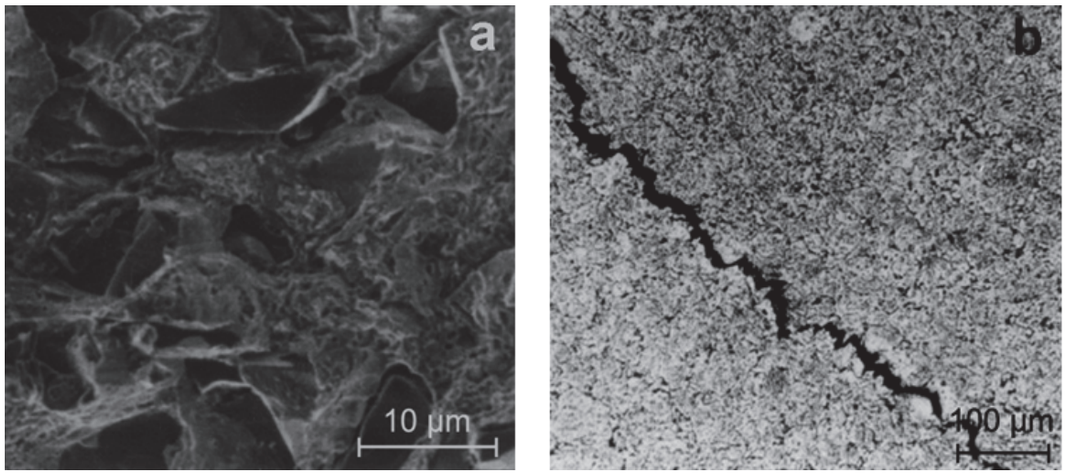


Fig. 20. Fracture surface of DRA materials after 60 min mixing. a) SEM. CW67- 10 vol.% SiC, d_{SiC}=10µm; b) LM. CW67- 10 vol.% SiC, d_{SiC}=10µm.

which block the propagating crack and deflect it. By deflecting the crack, the energy level at the crack tip which is necessary for its propagation decreases disabling its further propagation. Therefore, more energy (larger applied force) has to be introduced to the system for the continuation of crack movement. This fact explains why these, more homogenous alloys, have better mechanical properties (Fig. 22).

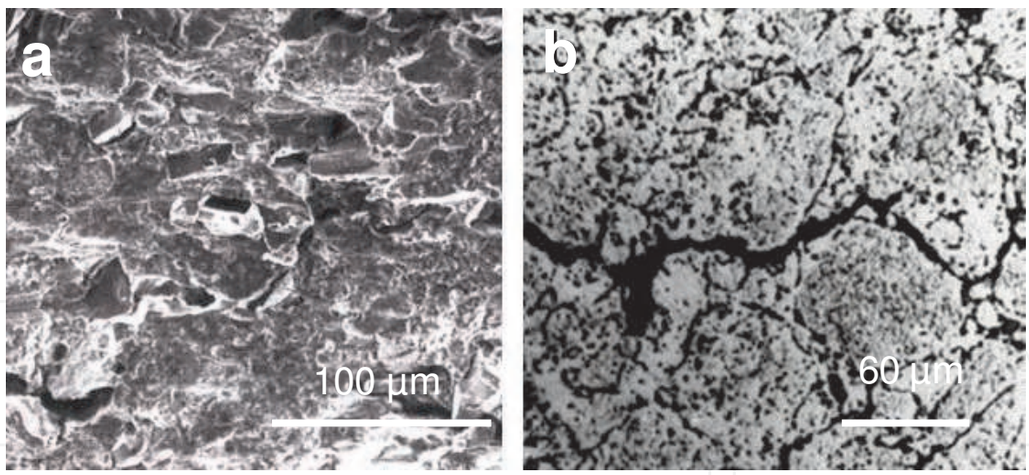


Fig. 21. Fracture surface of DRA materials after 60 min mixing. a) SEM. CW67- 10 vol.% SiC, d_{SiC}=15µm; b) LM. CW67- 5 vol.% SiC, d_{SiC}=0.7 µm.

In the case when the reinforcing particles are not evenly distributed in the alloy matrix, crack propagates easily through the matrix (Fig. 23 a and b). This behaviour corresponds to poor mechanical properties of the DRA material with such microstructure. When mixing time is too long a formation of SiC agglomerates is noticeable. Due to the very weak bonding between the SiC particles in the agglomerates, a particle decohesion will easily occur under applied stress and the crack will appear (Fig.24).

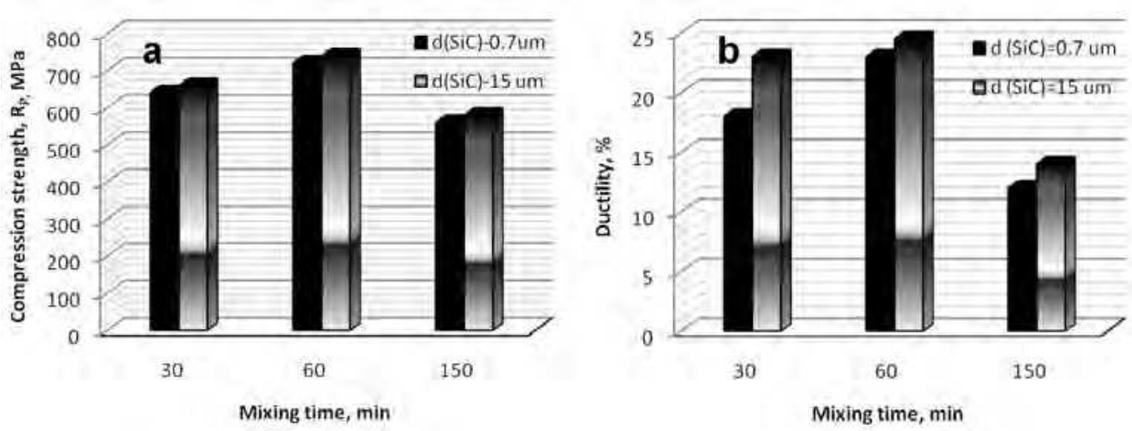


Fig. 22. CW67- 5 vol. % SiC composite compression properties dependence on time of mixing. a) compression strength; b) ductility.

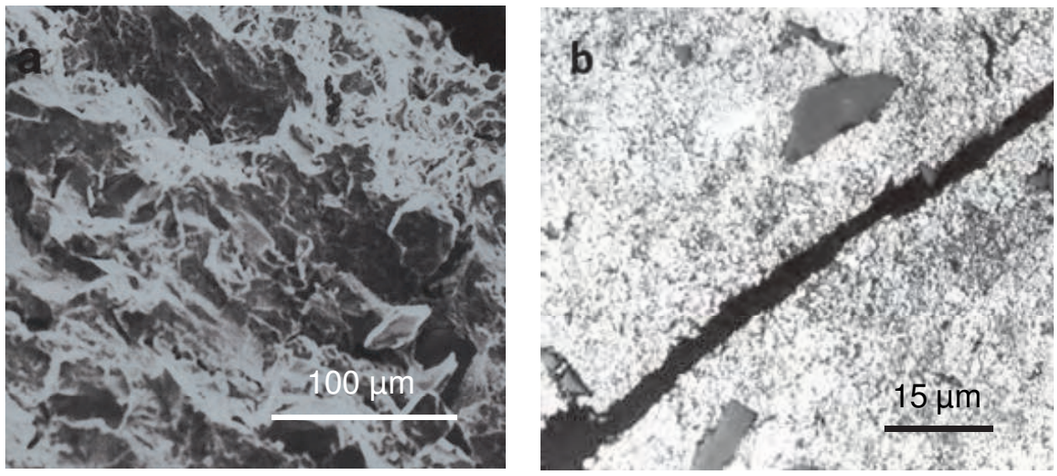


Fig. 23. Fracture surface of DRA material after 30 min mixing. a) SEM. CW67-10 vol.% SiC, d_{SiC}=15 µm and b) LM. CW67-10 vol.% SiC, d_{SiC}=15 µm.

As observed by Humphreys (1988), an addition of a brittle reinforcement phase in high strength aluminum alloys may even decrease the ultimate tensile strength. Indeed, in the present composites this was found to be the case. Indeed, in the present composites this was found to be the case. The values of the ultimate strength were lower than the values for the monolithic material (Table 3). The presence of SiC particles can be detrimental to the ultimate compressive strength of the composite materials because of more additional cracking mechanisms compared to monolithic alloy. These mechanisms are: particle cracking (Fig. 25), particle matrix debonding (Fig. 20 a) and particle agglomerate decohesion (Fig. 19). The latter two mechanisms are of a secondary importance when particles are well distributed and strongly bonded. Thus, it is particle cracking that has a major influence on the ultimate compressive strength of SiC/Al composite materials.

Extensive studies of the room temperature mechanical behavior of these composites have been conducted, but the information about mechanical properties of DRA materials at elevated temperatures is still limited. Therefore, some results of the temperature effect on

the compressive properties and fracture behaviour of a SiC particle reinforced CW67 aluminium alloy will be presented.

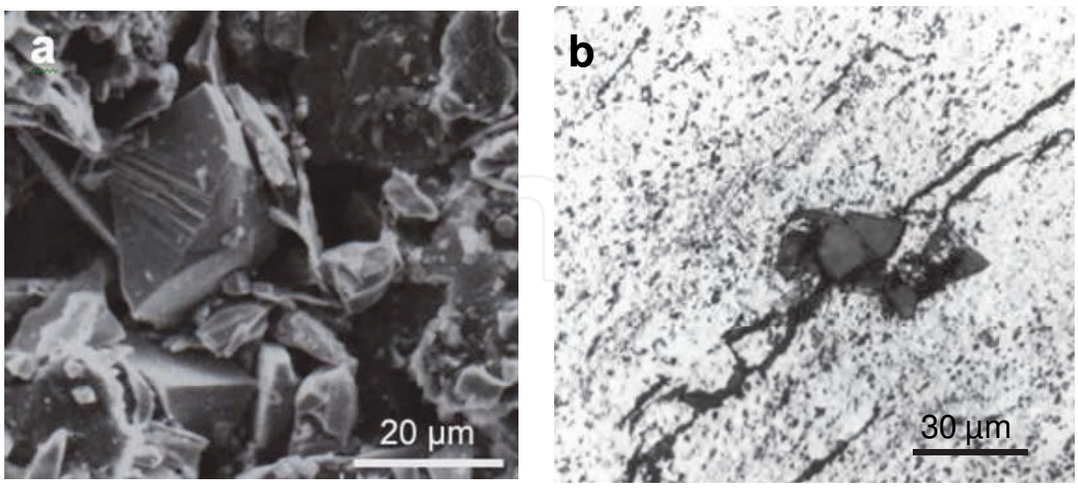


Fig. 24. Fracture surface of DRA material after 150 min mixing. a) SEM. CW67-5 vol.% SiC, d_{SiC}=15 µm; b) LM. CW67-5 vol.% SiC, d_{SiC}=15 µm.

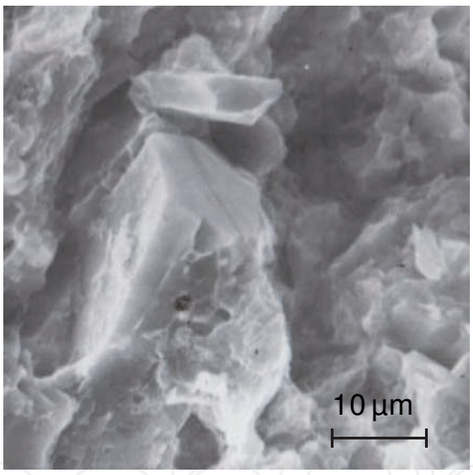


Fig. 25. SEM. Fracture surface of the composite with 15 vol.% SiC.

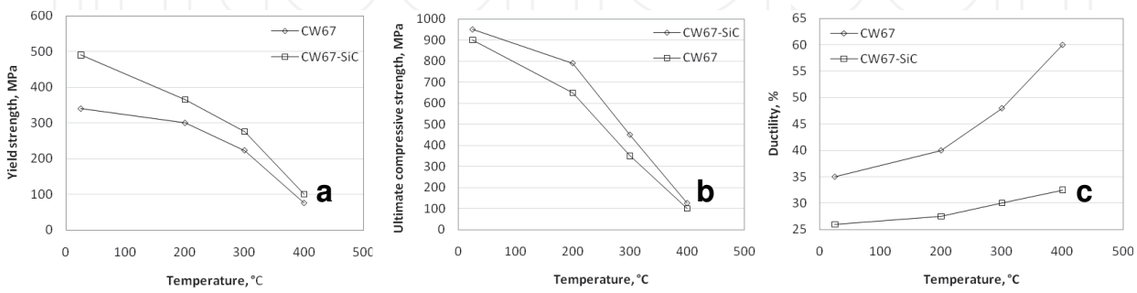


Fig. 26. a) to c) Compressive properties of CW67 and CW67- 15 vol. % SiC composite as a function of temperature.

With increasing temperature matrix becomes softer and stress accommodation around the particles caused by difference in CTE becomes easier compared to the room temperature. The constraint around the particles in the matrix can be relaxed by a dynamic recovery process. It is therefore expected that any misfit strain gradient can be relaxed by the recovery process which could lead to a decrease in work hardening and strength, resulting in a small difference in strength between the composite and the monolithic alloy at higher temperatures (Fig. 26 a, b). Increase of composite ductility with temperature (Fig. 26 c) can be a consequence of the improved ductility of the matrix. However, ductility of the composite is lower than that of the monolithic alloy, which is caused by the particle cracking or particle matrix debonding effects.

Microstructures of composites strained at room temperature show that SiC particles may fracture more frequently in the regions of agglomerates or by particle cracking of large particles, rather than by debonding between the matrix and SiC particles.

Presence of cavities is observed in microstructures of samples tested at elevated temperatures at the matrix/reinforcing phase interface (A in Figs. 27 and 28 b), particle boundaries (B in Fig. 27 b), and in the regions where the SiC particles are agglomerated (C in Fig. 27).

At 200˚C, small voids were found at the particle boundaries with tiny linkage between voids. At 300˚C and 400˚C these voids become larger. It has been observed (Fig. 27 a-c) that debonding between particles and the matrix accelerates above 200˚C.

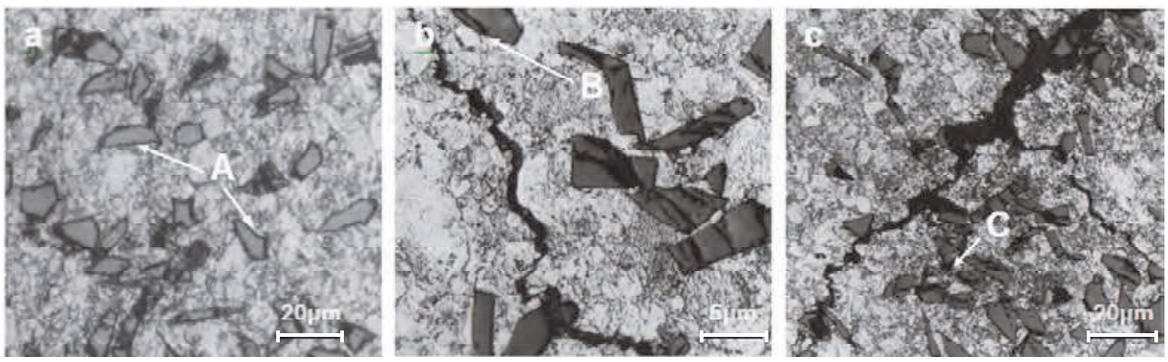


Fig. 27. LM. Longitudal sections of the composites tested at: a) 200°C, b) 300°C and c) 400°C.

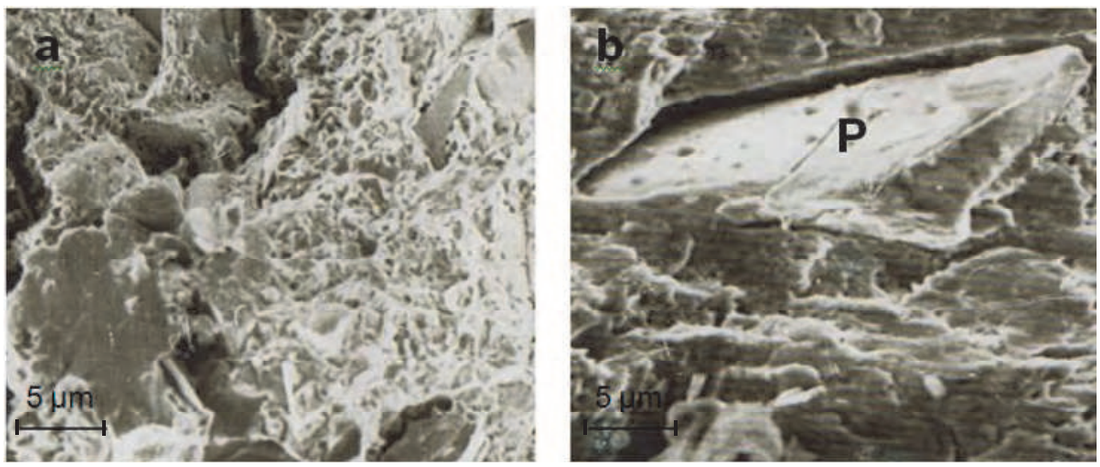


Fig. 28. SEM. a) and b) Fracture surface of the composite CW67-SiC tested at 400°C. (Mg, Cu)Zn_2 precipitates on SiC (indicated with P).

7. Conclusions

The basic conclusion is that much more research is needed for further enhancement of the DRA materials properties. Computer simulation and mathematical modeling of composite fabrication would enable faster achieving of results and therefore these methods need to be addressed. In this area some scattered work has been done but it still needs further development. By finding and establishing the proper models actual experimentation and prediction of properties, shape, size, volume fraction of the participating phases and mixing parameters would largely be cut down.

As mentioned before, dispersed phase size, shape, volume fraction, wettability and distribution play the most important role in the properties attained in metal-matrix composites. A lot of research is focused on optimizing these parameters and based on the results, property designing of composites is possible. However, all the experimentation has stopped at decreasing the dispersed phase level below 10μm, possibly due to the difficulty in dispersing uniformly and without coagulation of finer particles in the matrix. This is especially pronounced when the liquid metallurgy route is adopted for making the composites. If the coagulation problem cannot be solved when the particle size is decreased below 10 μm, alternate methods of fabrication have to be attempted. Most promising method so far, seems to be in-situ production of composites, which is recently a very modern trend in science. In the present age of nanomaterials, methods of dispersion or making composites with nano sized dispersed phase holds a lot of potential for commercial exploitation in the future.

8. Acknowledgements

Authors are in debt to the Ministry of Science of the Republic of Serbia for the financial support realized through the Project No. 172005.

9. References

Adler P.N., Delasi R., Geschwind G., Influence of microstructure on mechanical properties and stress-corrosion susceptibility of 7075 aluminum-alloy, *Metallurgical Transaction*, vol.3 12 (1972), pp. 3191-3200.

Bozic D., Pavlovic M., Mitkov M. and Nikacevic M., Mechanical and structural properties of CW67 alloy produced by powder metallurgy techniques (in Serbian), *Metalurgija* 3 (1997), p. 201.

Bozic D., Dimcic O., Dimcic B., Vilotijevic M., Riznic-Dimitrijevic S., Modeling of densification process for particle reinforced composites, *Journal of Alloys and Compounds*, vol. 487 1-2 (2009), pp. 511-516.

Doel T.J.A., Bowen P., Tensile properties of particulate-reinforced metal matrix composites, *Composites Part A*, vol. 27 8 (1996), pp.655-665.

Flom Y.and Arsenault R.J., Effect of particle size on fracture toughness of SiC/Al composite material, *Acta Metall* 37 (1989), pp. 2413–2423.

German R.M., *Powder Metallurgy Science,* Second Edition, 1994, Metal Powder Industries Federation, Princeton, NJ.

German R. M., *Sintering Theory and Practice*, John Wiley and Sons Inc., New York,NY; 1996

Gnjidić Ž., Božić D., *Tehnika,* vol. 8, 6 (1999), pp.5.

Gnjidić Ž., Božić D., and Mitkov M., The influence of SiC particles on the compressive properties of metal matrix composites, *Mater Charact* 47 (2001), pp. 129–138.

Gray W.A., *The packing of solid particles*, Champan and Hall Ltd., London (1973).

Humphreys F. J., In: *Proceedings in Mechanical and Physical behavior of metallic and ceramic composites*, ed. Anderson S et al. 51 (1988).

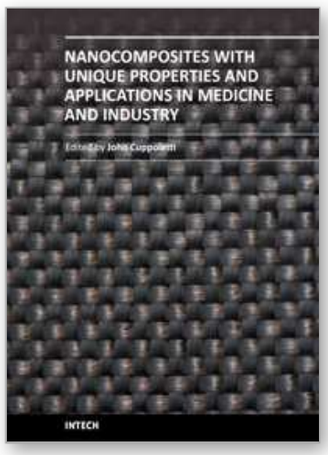
Mc Kimpson M.G., Heimi A.N., Hung X. In: *Proceedings of structural applications of mechanical alloying*, vol. 203. Materials Park, Ohio: ASM; 1999.

Miller W. S., Humphreys F. J., Strengthening mechanism in metal matrix composites, *Scripta Metall. Mater.* 25 (1991), pp.

Rees D.W.A., deformation and fracture of metal matrix particulate composites under combined loading, Composites, Part A, 1998, 29A: 171-82.

Tietz T.E. and Palmour G., *Advances in powder technology* vol. 9, ASM, Metals Park, Ohio (1986) p. 189.

IntechOpen



Nanocomposites with Unique Properties and Applications in Medicine and Industry

Edited by Dr. John Cuppoletti

ISBN 978-953-307-351-4
Hard cover, 360 pages
Publisher InTech
Published online 23, August, 2011
Published in print edition August, 2011

This book contains chapters on nanocomposites for engineering hard materials for high performance aircraft, rocket and automobile use, using laser pulses to form metal coatings on glass and quartz, and also tungsten carbide-cobalt nanoparticles using high voltage discharges. A major section of this book is largely devoted to chapters outlining and applying analytic methods needed for studies of nanocomposites. As such, this book will serve as good resource for such analytic methods.

How to reference

In order to correctly reference this scholarly work, feel free to copy and paste the following:

Dusan Bozic and Biljana Dimcic (2011). Synthesis and Properties of Discontinouosly Reinforced Aluminum Matrix Composites, Nanocomposites with Unique Properties and Applications in Medicine and Industry, Dr. John Cuppoletti (Ed.), ISBN: 978-953-307-351-4, InTech, Available from: http://www.intechopen.com/books/nanocomposites-with-unique-properties-and-applications-in-medicine-and-industry/synthesis-and-properties-of-discontinouosly-reinforced-aluminum-matrix-composites

INTECH
open science | open minds

InTech Europe
University Campus STeP Ri
Slavka Krautzeka 83/A
51000 Rijeka, Croatia
Phone: +385 (51) 770 447
Fax: +385 (51) 686 166
www.intechopen.com

InTech China
Unit 405, Office Block, Hotel Equatorial Shanghai
No.65, Yan An Road (West), Shanghai, 200040, China
中国上海市延安西路65号上海国际贵都大饭店办公楼405单元
Phone: +86-21-62489820
Fax: +86-21-62489821

© 2011 The Author(s). Licensee IntechOpen. This chapter is distributed under the terms of the Creative Commons Attribution-NonCommercial-ShareAlike-3.0 License, which permits use, distribution and reproduction for non-commercial purposes, provided the original is properly cited and derivative works building on this content are distributed under the same license.

IntechOpen

IntechOpen